Chemical Science

ROYAL SOCIETY OF CHEMISTRY

EDGE ARTICLE

View Article Online
View Journal

Cite this: DOI: 10.1039/d6sc03081e

All publication charges for this article have been paid for by the Royal Society of Chemistry

Aerobic C–H bond activation at a Pd center under aqueous conditions

Dae Young Bae, [a] Nicholas P. Ruhs[b] and Liviu M. Mirica *[a]

Recent reports have increasingly documented palladium-catalyzed C–H bond functionalization reactions involving high-valent Pd^{III} and Pd^{IV} intermediates, yet these transformations often depend on strong oxidants and external bases. Herein, we report a series of Pd^{II} complexes $[(^{PR}N3CH)Pd^{II}(MeCN)](BF_4)_2$, supported by a tetradentate pyridinophane ligand, that undergo aerobic C–H bond activation under mild aqueous conditions without the need for an added external base to generate isolable Pd^{III} complexes. In this transformation, O_2 serves as both an oxidant and proton acceptor, eliminating the need for an exogenous base. Mechanistic and computational studies are consistent with a rate-limiting concerted metalation–deprotonation (CMD) pathway involving a key Pd–O_2 species that promotes C–H bond activation. Notably, the presence of water in the solvent mixture and slightly elevated temperatures enhance reactivity and lead to quantitative formation of the Pd^{III} product, improving its synthetic utility. Overall, this study establishes a C–H bond activation pathway at high-valent palladium centers that proceeds without added external base, with O_2 serving as both oxidant and internal proton acceptor. These findings provide key insights into high-valent palladium reactivity and lay a mechanistic foundation for sustainable aerobic oxidation strategies.

Received 14th April 2026
Accepted 27th May 2026

DOI: 10.1039/d6sc03081e

rsc.li/chemical-science

Introduction

The importance and versatility of Pd-catalyzed C–H activation reactions in the synthetic community have been well documented over the past several decades.[1–7] More recently, oxidative C–H activation pathways involving high-valent Pd^{III} and Pd^{IV} intermediates have attracted significant attention.[1,8–13] In this context, our group has also explored C–H activation chemistry mediated by high-valent group 10 metal complexes supported by pyridinophane ligands.[14–20]

Despite these advances, most high-valent Pd-mediated C–H activation systems rely on strong chemical oxidants and an external base, raising concerns regarding sustainability and functional group compatibility.[21,22] A major challenge in high-valent Pd chemistry is the development of mild and sustainable oxidation strategies that eliminate the need for hazardous reagents, while maintaining mechanistic control over product formation. Molecular oxygen represents an attractive terminal oxidant owing to its abundance and environmental compatibility especially in Pd-catalyzed C–H functionalization.[23–34] Notably, the Yu group has reported several prominent examples of Pd-catalyzed C–H functionalization reactions, utilizing O_2 as an oxidant across a broad range of reactions.[31,35–37] However, most O_2-based Pd^{II} systems still require an external base, typically acetate, to facilitate C–H bond activation.[35,36] Developing a system that operates without an added external base, in which O_2 serves as both the oxidant and the proton acceptor, would represent a significant conceptual advance. Water is an appealing medium in this regard due to its abundance and hydrogen-bonding properties,[38–42] however, its role in high-valent Pd-mediated aerobic C–H bond activation remains poorly understood.[36,43–48] Additionally, previously reported O_2/H_2O systems often require elevated temperatures or prolonged reaction times, limiting their practicality, and key mechanistic details including the interaction between Pd and O_2 and the nature of the transient high-valent Pd/O_2 intermediates remain unresolved.[38,49]

Several studies have described aerobic C–H bond activation at Pd centers in the absence of an external base (Fig. 1). For example, Vilar and coworkers demonstrated that a Pd^{I} dimer reacts with O_2 to form a C–O bond *via* C–H bond activation, although the yield of the Pd^{II} product and the fate of the C–H-derived hydrogen atom were not fully clarified (Fig. 1a).[50] The Goldberg group reported aerobic oxidation of a Pd^{0} complex to a Pd^{II}-peroxo species, which subsequently promotes C–H activation through a cyclometalated Pd–OOH intermediate (Fig. 1b).[51] Our group has also reported Pd^{II} complexes that activate C–H bond aerobically through high-valent Pd intermediates (Fig. 1c),[18] in addition to aerobically-induced C–C or C–O bond formation reactions *via* high-valent Pd species.[52–56] While these studies establish the feasibility of aerobic C–H bond activation at Pd, detailed insights into how O_2 interacts with Pd and the C–H

[a]*Department of Chemistry, University of Illinois at Urbana-Champaign, 600 S. Mathews Avenue, Urbana, Illinois 61801, USA. E-mail: mirica@illinois.edu*

[b]*Department of Chemistry, Washington University in St. Louis, One Brookings Drive, St. Louis, Missouri 63130-4899, USA*

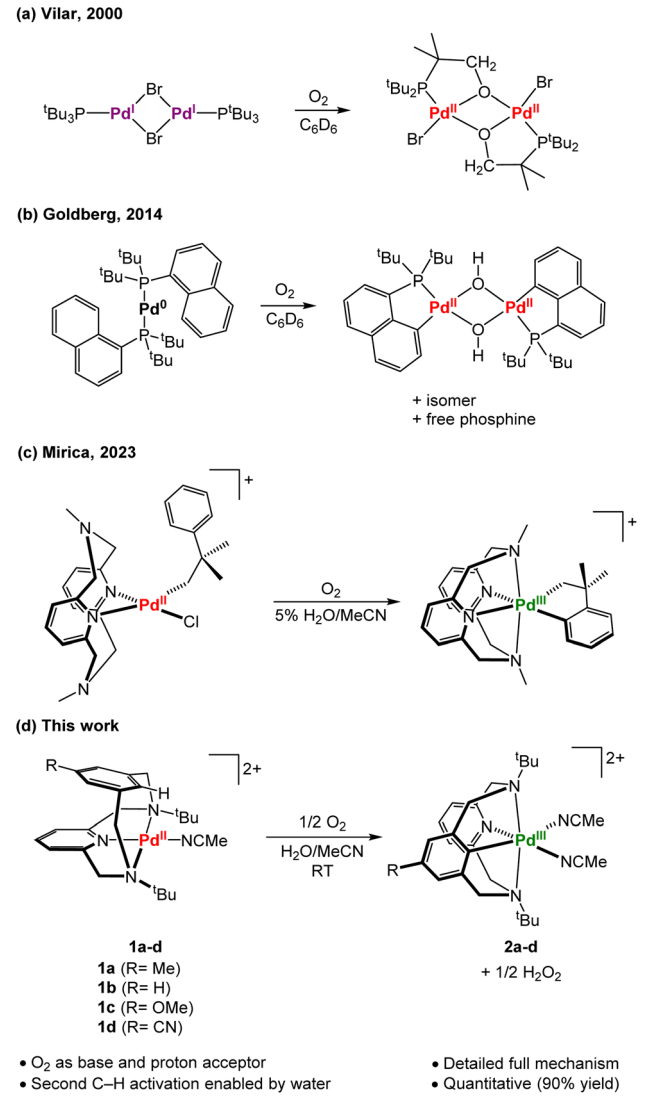

Fig. 1 (a–c) Reported aerobic C–H bond activation without an added external base by Pd species from Vilar,[50] Goldberg,[51] and Mirica[18] groups; (d) the reaction of complexes **1a–d** under aerobic conditions reported in this study.

substrate without an exogenous base remain limited. In addition, most reported systems rely on low-valent Pd complexes supported by electron-rich ligands that readily react with O_2. The product yields are typically low, and the fate of the protons and oxygen atoms have rarely been clarified.

Herein, we report the aerobic C–H bond activation of Pd^{II} complexes, $[(^{pR}N3CH)Pd^{II}(MeCN)](BF_4)_2$, **1a–d**, at room temperature in aqueous solution, proceeding without exogeneous base to afford isolable Pd^{III} complexes $[(^{pR}N3C)Pd^{III}(MeCN)_2](BF_4)_2$, **2a–d**, in quantitative yield (Fig. 1d). While the Pd^{III}-aryl complex has been previously reported by our group,[15] its formation *via* direct O_2-mediated C–H activation and the quantitative kinetic and mechanistic framework for this transformation have not been previously reported. Combined kinetic, mechanistic, and computational studies establish that a Pd^{III}-superoxo intermediate promotes C–H bond activation through a CMD-like transition state in which a Pd/O_2 species functions as an internal base. Moreover, hydrogen bonding in water lowers the barrier for C–H bond activation steps, enabling pathways inaccessible in non-aqueous media. Use of slightly elevated temperatures shortens the reaction time to ~1 hour, rendering the use of oxygen as an oxidant and proton acceptor more practical. Overall, these findings reveal a mechanistically distinct aerobic C–H bond activation pathway at high-valent Pd centers, with broad implications for the design of future sustainable oxidation strategies.

Results and discussion

Synthesis and characterization of 1a

The $[(^{pMe}N3CH)Pd^{II}(MeCN)](BF_4)_2$ (**1a**) complex was prepared in 85% yield *via* the reaction of $^{pMe}N3CH$ and $[Pd^{II}(MeCN)_4](BF_4)_2$, and X-ray quality orange-colored crystals of **1a** could be obtained from vapor diffusion of diethyl ether into acetonitrile solution at −35 °C. The structure of **1a** reveals a square planar geometry around the Pd center ($\tau_4 = 0.12$), with one pyridine nitrogen atom, two amine atoms, and one nitrogen atom from one MeCN (Fig. 2). Interestingly, the Pd···H1 distance is 2.393 Å, which is much shorter than in the previously reported complex $(^{pMe}N3CH)Pd^{II}(OAc)_2$ (2.81 Å),[15] and thus suggesting a stronger Pd···H–C_{ipso} interaction. The ^{1}H NMR spectrum of **1a** reveals a distinct peak attributed to the C_{ipso}–H proton at 9.45 ppm, which was shifted downfield compared to 7.08 ppm in the free ligand (Fig. S5),[15] implying that the Pd···H–C interaction can be defined as a weak anagostic interaction.[57] The close interaction of the C–H bond with the Pd^{II} center is likely due to a ligand enforced geometry around the metal center,[57–61] while the broad peaks of the methylene groups in the ^{1}H NMR spectrum indicate the complex is fluxional in solution (Fig. S5). Notably, in the same crystal batch of complex **1a** a small amount of yellow crystals were found and determined to correspond to the di-solvento complex $[(\kappa^2\text{-}^{pMe}N3CH)Pd^{II}(MeCN)_2](BF_4)_2$ (**1ab**, Fig. S49), reminiscent of the previously reported $(^{pR}N3CH)Pd^{II}(OAc)_2$ complexes, and further supporting the fluxional nature of the pyridinophane ligand that can support various

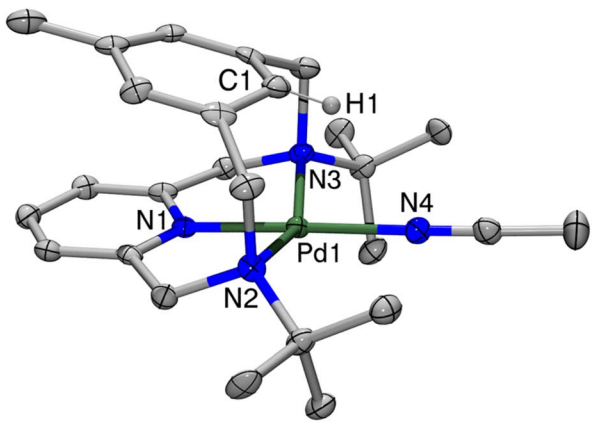

Fig. 2 Solid-state structure of dication of **1a** with 50% probability ellipsoids. The counterions and hydrogen atoms were omitted for clarity. Selected bond distances (Å) and angles (°): Pd1–N1 1.947(5), Pd1–N2 2.210(6), Pd1–N3 2.201(6), Pd1–N4 2.011(5), Pd1–H1 2.393, Pd1–C1 2.563(7), Pd1–H1–C1 89.3.

coordination geometries around the Pd center.[15] Finally, the cyclic voltammogram (CV) of **1a** exhibits an irreversible anodic peak at $E_{pa,ox} = 1.09$ V *vs.* $Fc^{+/0}$ and a reversible reductive wave at $E_{1/2,red} = -0.43$ V *vs.* $Fc^{+/0}$ (Fig. S15). The irreversible anodic peak is tentatively attributed to oxidation of the Pd^{II} precursor, and the reversible reductive wave is tentatively assigned to the $Pd^{I/II}$ redox process. The relatively high oxidation potential may stem from a structural change at the Pd center that is needed to stabilize the Pd^{III} center.[62–64]

Oxidative reactivity of 1a

To investigate C–H bond activation *via* a high-valent Pd pathway, we examined the oxidative reactivity of **1a** using various oxidants. The addition of $^{Ac}FcPF_6$ (+0.25 V *vs.* $Fc^{+/0}$),[65] $NOBF_4$ (+0.87 V *vs.* $Fc^{+/0}$),[65] (thianthrenyl)BF_4 (+0.86 V *vs.* $Fc^{+/0}$),[65] or $PhICl_2$ (−0.9 V *vs.* $Fc^{+/0}$)[66] to a solution of **1a** did not yield any detectable high-valent Pd species, and instead decomposition to Pd black was observed. In contrast, exposure of **1a** to O_2 (+0.68 V *vs.* $Fc^{+/0}$)[67] or air in MeCN led to the formation of the Pd^{III} complex $[(^{pMe}N3C)Pd^{III}(MeCN)_2](BF_4)_2$ (**2a**, Fig. 1d), as confirmed by UV-Vis and EPR spectroscopy (Fig. 3a and S18). While the employed oxidants are likely not oxidizing enough to oxidize **1a** (+1.09 V *vs.* $Fc^{+/0}$, Fig. S15) *via* outer-sphere oxidation, O_2 appears to promote C–H bond activation through a distinct inner-sphere pathway likely involving coordination to Pd, ligand exchange, and structural reorganization steps. Moreover, this transformation represents a rare example of aerobically promoted C–H bond activation occurring without an added external base.

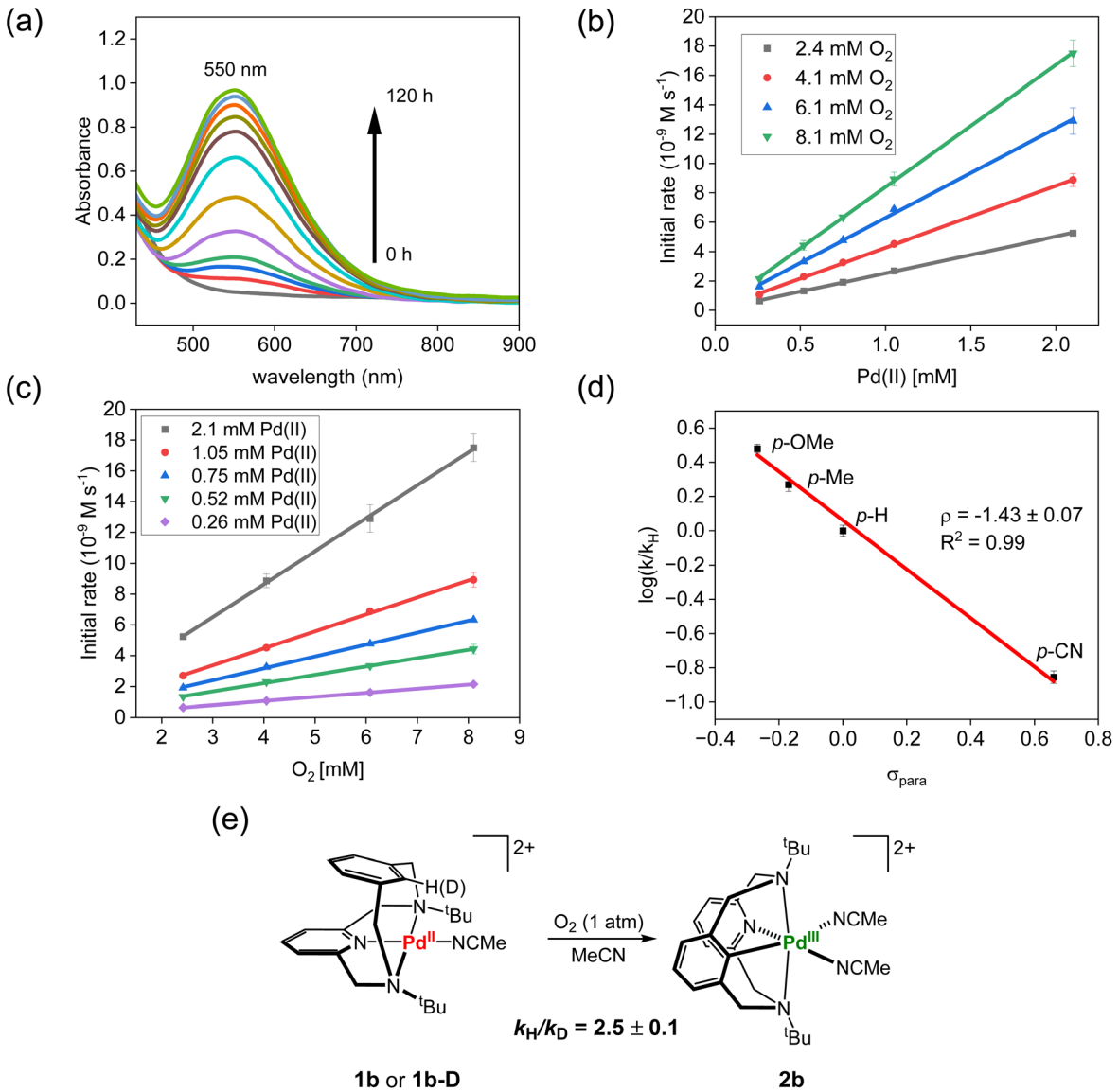

Fig. 3 (a–c) Kinetic analysis of aerobic C–H bond activation of complex **1a** in MeCN at 293 K: (a) UV-Vis monitoring of the formation of **2a**, with a characteristic absorption band at 550 nm, upon the reaction of **1a** (1.05 mM) with O_2 (8.1 mM), (b) Pd^{II} dependence ($[O_2] = 2.4–8.1$ mM), and (c) O_2 dependence ($[Pd^{II}] = 0.26–2.1$ mM). (d) Hammett analysis of the aerobic C–H bond activation reactions for *para*-substituted complexes **1a–d** (1.05 mM) in O_2-saturated MeCN (8.1 mM) at 293 K. (e) Kinetic isotope effect determined by independent rate measurements of **1b** (1.05 mM) and **1b-D** (1.05 mM) in O_2-saturated MeCN (8.1 mM) at 293 K.

A structurally related Pd^{II}-acetate complex (^{pMe}N3CH)$Pd^{II}(OAc)_2$, which shares the same ligand scaffold as **1a**, did not undergo C–H bond activation under aerobic conditions, even in the presence of excess acetate.[15] The X-ray crystal structure suggests that the binding of the two acetate ligands prevents the positioning of the C–H bond in the proximity of the Pd center for activation. In contrast, complex **1a** features a labile MeCN ligand and adopts a geometry that allows for a shorter Pd···H_{ipso} distance, 2.393 Å *vs.* 2.808 Å in (^{pMe}N3CH)$Pd^{II}(OAc)_2$, and thus facilitating the O_2-mediated C–H bond activation. Overall, these observations highlight the crucial role of ligand substitution and structural flexibility in enabling aerobic C–H bond activation.

Kinetics on the aerobic reactivity of 1a

In order to probe the mechanism of this transformation and the specific role of O_2 during C–H bond activation, we conducted kinetic studies on the aerobic oxidation of [(^{pR}N3CH)Pd^{II}(MeCN)]$(BF_4)_2$ complexes **1a–d**. For consistency, the kinetic studies were performed using *in situ* generated complexes by mixing 1 equiv. $Pd(MeCN)_4(BF_4)_2$ with 1 equiv. of ^{pR}N3CH ligand; the detailed experimental procedures are provided in the SI. We tracked the formation of the product **2a–d** by monitoring the development of the absorbance at 550 nm in UV-Vis (Fig. 3a). The kinetic order of the Pd^{II} complex (**1a**) and oxygen was investigated (Fig. 3b and c). The absorbance peak corresponding to **2a** at 550 nm gradually increased and reached saturation after 96 hours (Fig. S20). As the reaction proceeded slowly, the rates of reaction were determined using the method of initial rates,[68] to reveal a first-order dependence on [Pd^{II}] at various O_2 concentrations in MeCN (Fig. 3b, [O_2] = 2.4–8.1 mM).[69,70] In addition, first-order kinetics in O_2 was observed at all Pd concentrations (Fig. 3c, [Pd^{II}] = 0.26–2.10 mM). Based on the experimental results that the reaction is first-order kinetics in both [Pd^{II}] and [O_2], we conclude that the reaction follows second-order kinetics overall. To ensure the reliability of the initial rate analysis, we additionally performed global kinetic fitting using a second-order rate model with respect to **1a** (Fig. S29). The fitting was conducted using the entire time course of the reaction (>3 $t_{1/2}$), giving a rate constant of $k_{global} = 1.01 \times 10^{-3}$ M^{-1} s^{-1}. The value is in good agreement with that obtained from the initial rate method ($k_{initial} = 1.05 \times 10^{-3}$ M^{-1} s^{-1}), and the fitted curve reasonably reproduces the experimental kinetic trace for the formation of product **2a**. In addition, the rate constants obtained under various Pd^{II} and O_2 concentrations remain consistent, further supporting the validity of the initial rate method (Fig. S7). Given the similar kinetic parameters obtained from initial rate analysis and global kinetic fitting, for simplicity the initial rate method was employed for most kinetic analyses, and all detailed kinetic procedures and fitting methods are provided in the SI.

Hammett ρ and kinetic isotope effect (KIE) studies

We next sought to study the electronic dependence of the aerobic oxidation reaction. By comparing the reaction rates of the system described above with those of the modified N3CH analogs, we aimed to evaluate the extent to which *para*-substituents on the reactive C–H bond influence the reaction rate and to elucidate the underlying reaction mechanism. A Hammett analysis was performed by comparing the rates obtained at a Pd concentration of 1.05 mM and O_2 concentration of 8.1 mM (Fig. 3d). A ρ value of -1.43 ± 0.07 was obtained with a strong correlation ($R^2 = 0.99$), indicating that electron-donating substituents accelerate the reaction. The negative ρ value is consistent with the development of positive charge in the transition state.

To gain further mechanistic insight, the kinetic isotope effect (KIE) was examined for the reactions of **1b** and **1b-D**, in which the H_{ipso} of **1b** was replaced by deuterium. A primary KIE value of $k_H/k_D = 2.5 \pm 0.1$ was obtained (Fig. 3e). This experimentally determined KIE indicates that C–H bond activation contributes to the rate-limiting in this transformation.[71]

The experimentally determined Hammett and KIE values are consistent with those reported for acetate-assisted Pd-mediated C–H bond activation reactions.[72–79] In particular, the observed primary KIE (~2.5) and the Hammett correlation support the involvement of a concerted metalation–deprotonation (CMD)-type C–H activation step. Notably, in contrast to previously reported acetate-assisted systems, the present reaction proceeds without an added external base. These results are therefore consistent with a scenario in which oxygen-derived ligands, such as superoxide or hydroperoxide, function as internal bases and participate in proton abstraction during C–H activation.

Optimized C–H bond activation under aqueous conditions

Complex [(^{pMe}N3C)Pd^{III}(MeCN)$_2$]$(BF_4)_2$ (**2a**) was independently synthesized and fully characterized, enabling accurate determination of product yields by UV-Vis spectroscopy (ε_{550nm} = 2128 M^{-1} cm^{-1} in MeCN, 2148 M^{-1} cm^{-1} in 9 : 1 H_2O : MeCN; Fig. S17). Under aerobic conditions in neat acetonitrile, formation of **2a** was limited to ~46% yield. To improve both the reaction efficiency and rate, solvent mixtures containing water were examined. Notably, increasing the proportion of water led to a marked enhancement in reactivity, with the yield of **2a** reaching up to 90% in a 9 : 1 H_2O : MeCN mixture (Fig. 4, S27 and Table S11).[52,53,55,80] Reaction rates were also significantly accelerated under aqueous conditions, with complete conversion achieved within 1.5 h at 70 °C (Fig. S28, Tables S12 and S13). These results highlight the unusually mild nature of this aerobic C–H bond activation, which proceeds without an added external base, compared to typical aerobic C–H functionalization reactions that require higher temperatures and longer reaction times.[24,29,31,34–37,49]

To probe the stoichiometric role of O_2 in this transformation, reactions of **1a** were conducted using varying equivalents of O_2 (Fig. S32). In 9 : 1 H_2O : MeCN, exposure of 1 or 0.5 equivalents of O_2 afforded the C–H activated Pd^{III} complex **2a** in 83% and 79% yield, respectively, whereas use of 0.25 equivalents of O_2 resulted in approximately 50% yield of **2a**. These observations indicate that O_2 functions as a two-electron oxidant in this system.[81–83] Consistent with this assignment, simultaneous formation of hydrogen peroxide was detected spectrophotometrically,[84–86] with the reaction of **1a** (1.05 mM) and excess O_2 in 9 : 1 H_2O : MeCN producing **2a** in 90% yield

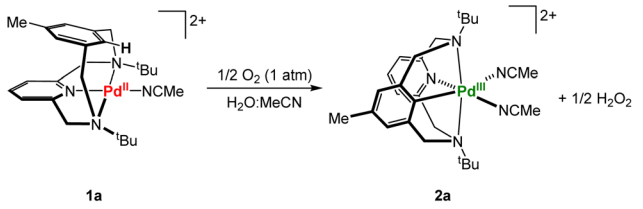

Fig. 4 Yield comparison of product **2a** and byproduct H_2O_2 during the reaction of **1a** with O_2 in two different H_2O : MeCN solvent mixture ratios.

along with H_2O_2 in ~42% yield. In contrast, under otherwise identical conditions in neat acetonitrile, formation of H_2O_2 was negligible (<3%), and the yield of **2a** remained limited to ~46%. These results suggest that while the initial C–H bond activation is accessible in both solvents, the subsequent C–H bond activation step is strongly suppressed in pure MeCN. As a consequence, the overall reaction in neat acetonitrile terminates after formation of approximately half an equivalent of the C–H activated Pd^{III} complex. By comparison, under aqueous conditions, both the initial and subsequent C–H bond activation steps proceed, resulting in the formation of one equivalent of **2a** and half an equivalent of H_2O_2 per equivalent of **1a**. The origin of this pronounced solvent dependence is addressed through computational analysis (*vide infra*). Under 9 : 1 H_2O : MeCN conditions, the full time-course data (>3 $t_{1/2}$) were also analyzed by second-order global nonlinear fitting with explicit consideration of the overall reaction stoichiometry. The resulting rate constants at each temperature closely match those obtained from the corresponding initial rate analysis (see SI), confirming the validity of the second-order kinetic treatment.

To further probe the nature of the rate-determining step, an Eyring analysis was conducted under aqueous conditions over the temperature range of 20–70 °C (Fig. S31). The resulting activation parameters ($\Delta H^{\ddagger} = 16.7$ kcal mol^{-1} and $\Delta S^{\ddagger} = -11.8$ cal mol^{-1} K^{-1}) correspond to a $\Delta G^{\ddagger}$ of 20.2 kcal mol^{-1} at 20 °C. The negative entropy of activation, together with the observed second-order kinetics, is consistent with a bimolecular, associative transition state, in which O_2 and the Pd^{II} complex interact during the rate-determining C–H bond activation step.[87–91] Based on these kinetic observations, we propose the following mechanism for the aerobic C–H bond activation of **1**.

Proposed mechanism and rate law for the aerobic oxidation of 1

Based on our experimental observations and by analogy to acetate-assisted cyclopalladation reactions,[92] we propose a mechanism for the aerobic oxidation of **1** (Fig. 5) under aqueous conditions. Oxidation of the Pd^{II} complex **1** by O_2 generates a Pd^{III}-superoxide intermediate (**Int1**), which is expected to form reversibly and be present in trace amount under the reaction conditions. The Pd^{III}-superoxide species subsequently undergoes C–H bond activation *via* transition state **TS1**, which constitutes the rate-determining step of the reaction. The observed second-order kinetics, KIE, and Eyring analysis are all consistent with C–H bond activation being rate-limiting. The negative Hammett ρ value further supports an electrophilic-type transition state, consistent with a concerted C–H bond activation pathway. Following this step, a high-valent Pd^{IV}-hydroperoxide intermediate (**Int2**) is formed, which undergoes rapid comproportionation and ligand exchange with another equivalent of **1** to generate the C–H activated product **2** and a Pd^{III}-hydroperoxide species (**Int3**).[52,53,93,94]

In the presence of water, the Pd^{III}-hydroperoxide intermediate undergoes a subsequent, faster C–H bond activation to

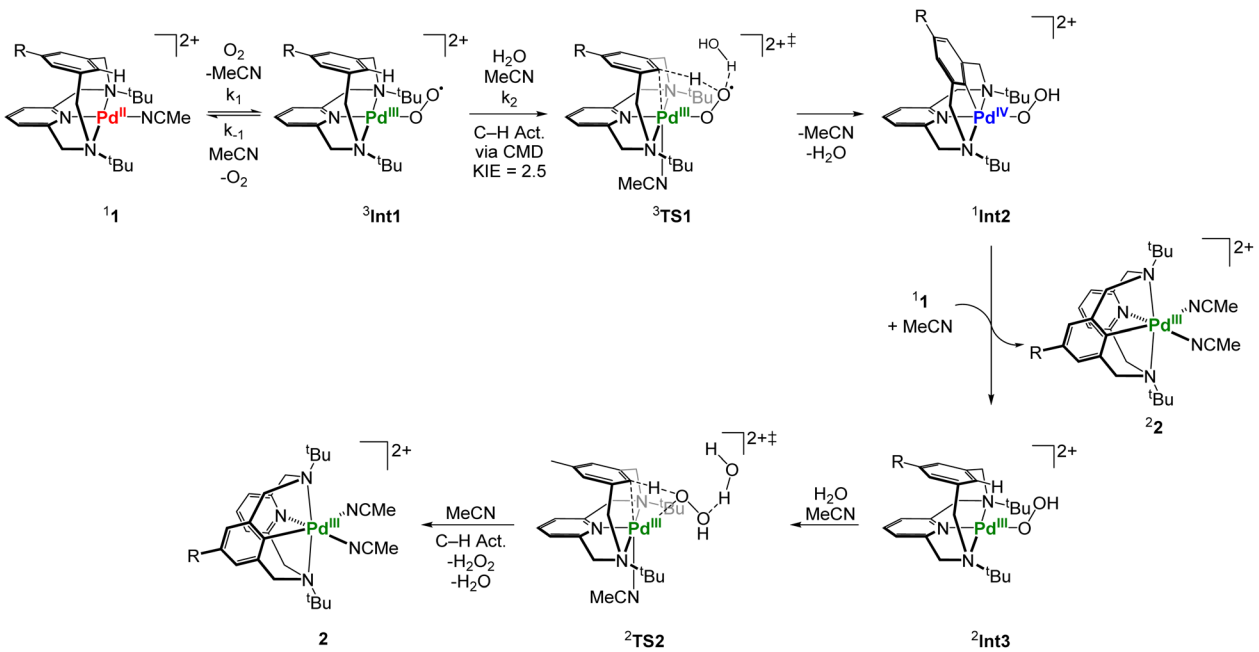

Fig. 5 Proposed mechanism for the aerobic oxidation of **1** under aqueous conditions.

(1) **1** + O_2 $\underset{k_{-1}}{\overset{k_1}{\rightleftharpoons}}$ **Int1** (fast, steady-state)

(2) **Int1** $\xrightarrow{k_2}$ **Int2** (RDS, C–H bond activation)

$$\text{rate} = \frac{k_1 k_2}{k_{-1} + k_2}[\mathbf{1}][O_2]$$

Scheme 1 Proposed kinetic model for the aerobic oxidation of **1** analyzed using the steady-state approximation.

afford an additional equivalent of **2** with concomitant formation of hydrogen peroxide. Notably, this pathway is significantly suppressed in pure MeCN, accounting for the solvent-dependent product yields observed experimentally. To further evaluate the proposed mechanism, a rate law was derived using a steady-state treatment of ^{3}**Int1** (Scheme 1). The resulting expression predicts first-order dependence on both [**1**] and [O_2], consistent with the experimentally observed kinetic data.

While the experimental data are consistent with a CMD-like C–H bond activation pathway, operating without an added external base, additional insight into the elementary steps was sought through computational studies.

Computational investigation of C–H bond activation without an exogenous base

To validate the experimentally proposed CMD-like C–H bond activation mechanism operating without an added external base, density functional theory (DFT) calculations were performed (Fig. 6). These calculations were designed to define the electronic structure of the oxygen-bound intermediates, identify the rate-determining step, and rationalize the experimentally observed solvent-dependent reactivity.

The reaction pathway begins with oxidation of the Pd^{II} species **1a** to generate an oxygen-bound Pd intermediate, upon replacement of the coordinated acetonitrile with O_2. Multiple electronic formulations and binding modes were evaluated computationally, including a singlet Pd^{III}-superoxo species (^{1}**Int6**, 35.7 kcal mol^{-1}), a Pd^{IV}-peroxo species (^{1}**Int5**, 28.5 kcal mol^{-1}; Fig. S53), and the triplet Pd^{III}-superoxo complex ^{3}**Int1**. Among these possibilities, the Pd^{III}-superoxo complex ^{3}**Int1** was identified as the lowest-energy intermediate (11.9 kcal mol^{-1}), lying 16.6 kcal mol^{-1} below the corresponding Pd^{IV}-peroxo species. These results indicate that the triplet Pd^{III}-superoxo (^{3}**Int1**) provides the most favorable electronic structure under the present reaction conditions.

The possibility of a binuclear Pd-oxygen intermediate species was also considered. Although the present calculations do not categorically exclude all possible binuclear pathways, our

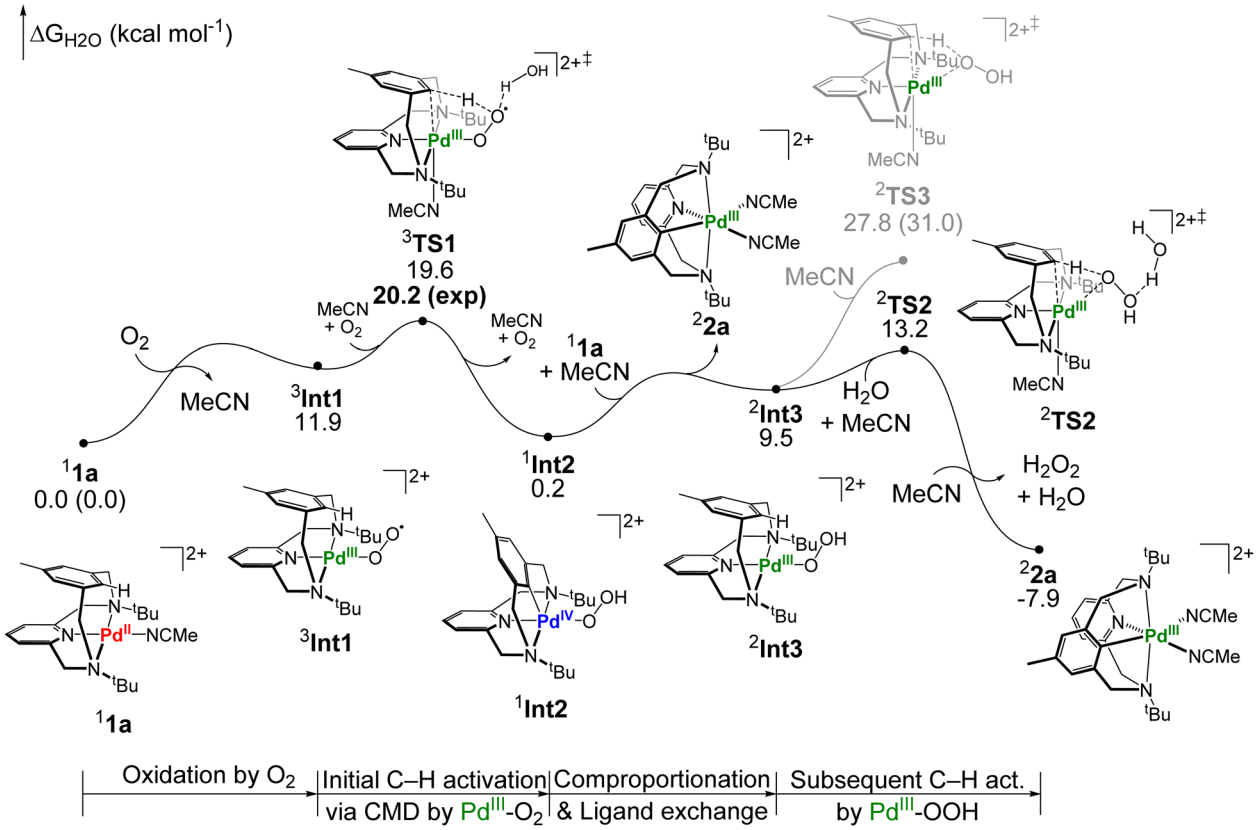

Fig. 6 Computed energy profile for the aerobic C–H bond activation of **1a** promoted by O_2 to generate the Pd^{III} product **2a** under aqueous conditions. Gibbs energies were calculated using the solvent model density (SMD) method in water, with selected energies for ^{1}**1a** and ^{2}**TS3** in MeCN shown in parentheses. The experimentally measured $\Delta G^{\ddagger}$ at 293 K for the overall C–H bond activation process is shown in bold under the calculated Gibbs energies for ^{3}**TS1**.

computational survey did not identify a binuclear oxygen-bound structure competitive in energy with the mononuclear Pd^{III}-superoxo species ^{3}**Int1**. This computational assessment is also consistent with the experimentally observed first-order dependence on [Pd] under the examined conditions, which would not support a binuclear pathway involving association of two Pd centers prior to or during the rate-limiting C–H activation step. Accordingly, the available kinetic and computational data are most consistent with assignment of ^{3}**Int1** as the initial Pd-oxygen intermediate in the proposed mechanism.

In the Pd^{III}-superoxo complex ^{3}**Int1**, the distal oxygen atom of the superoxo ligand is positioned to engage the H_{ipso} hydrogen, enabling a concerted C–H bond activation through transition state ^{3}**TS1** ($\Delta G^{\ddagger} = 19.6$ kcal mol^{-1}). The geometry and electronic structure of ^{3}**TS1** are characteristic of a CMD-like process, in which the superoxo ligand functions as an internal base to abstract the proton concomitant with Pd–C bond formation. Hydrogen bonding between a water molecule and the distal oxygen atom of the superoxo ligand in ^{3}**TS1** facilitates the initial C–H activation, resulting in a lower activation free energy compared to non-hydrogen bonded transition state ^{3}**TS4** (25.9 kcal mol^{-1}, Fig. S53). Passage through this transition state leads directly to formation of a high-valent Pd^{IV}-hydroperoxo intermediate (^{1}**Int2**).[52,53,55,56,95] Notably, the computed activation barrier for this step closely matches the experimentally derived barrier from Eyring analysis ($\Delta G^{\ddagger}_{obs} = 20.2$ kcal mol^{-1} at 20 °C), confirming that the initial C–H bond activation constitutes the rate-determining step of the overall reaction.

Following the first C–H bond activation, ligand exchange and facile comproportionation between the Pd^{IV}-hydroperoxo intermediate ^{1}**Int2** and an additional equivalent of the Pd^{II} reactant **1a** afford the C–H activated Pd^{III} product **2a** along with a Pd^{III}-hydroperoxide species (^{2}**Int3**) While this step is energetically accessible, further C–H bond activation from ^{2}**Int3** is highly sensitive to solvent effects.

In the presence of water, the Pd^{III}-hydroperoxide intermediate ^{2}**Int3** undergoes a subsequent C–H bond activation *via* transition state ^{2}**TS2** ($\Delta G^{\ddagger} = 13.2$ kcal mol^{-1}), yielding an additional equivalent of product **2a** with concomitant formation of hydrogen peroxide. In ^{2}**TS2**, hydrogen bonding between a water molecule and the distal oxygen atom of the hydroperoxide ligand significantly stabilizes the transition state, resulting in a substantial reduction of the activation barrier. By contrast, the corresponding water-free transition state ^{2}**TS3** exhibits a much higher barrier ($\Delta G^{\ddagger} = 27.8$ kcal mol^{-1}), and the barrier increases further under pure MeCN conditions ($\Delta G^{\ddagger} = 31.0$ kcal mol^{-1}). The pronounced energetic difference ($\Delta\Delta G^{\ddagger} = 14.6$ kcal mol^{-1}) accounts for the experimentally observed solvent dependence, wherein significantly higher yields of **2a** are obtained under aqueous conditions (9 : 1 H_2O : MeCN, 90%) compared to pure MeCN (46%), where the subsequent C–H bond activation is largely suppressed.

The stabilizing role of hydrogen bonding in facilitating hydroperoxide-mediated reactivity is consistent with prior observations in related systems, where interaction with the distal oxygen of the hydroperoxide ligand has been shown to promote bond activation.[96] To assess whether water could alternatively function as a proton shuttle during the subsequent C–H bond activation, additional pathways involving explicit proton transfer through water were evaluated (Fig. S53).[97] However, the computed activation barriers for these pathways ($\Delta G^{\ddagger} = 28.6$ kcal mol^{-1} for ^{2}**TS8** and ^{2}**TS9**) were comparable to that of the water-free transition state ^{2}**TS3**, indicating that proton shuttling does not significantly lower the barrier in this system.

Overall, the computational results are consistent with the experimental observations and support an aerobic C–H bond activation mechanism in which a Pd–O_2 species serves as a proton acceptor, without the need for an added exogeneous base. The calculations establish that the CMD-like C–H bond activation by a Pd^{III}-superoxo species constitutes the rate-determining step, while solvent-enabled hydrogen bonding plays a decisive role in lowering the barrier for C–H bond activations. These insights collectively rationalize the observed kinetics, solvent effects, and product distributions under aerobic conditions.

Conclusions

Herein, we report an aerobic C–H bond activation without an exogenous base mediated by the Pd complex [(^{pR}N3CH)Pd^{II}(MeCN)]$(BF_4)_2$, **1**, under aqueous conditions at room temperature, affording the Pd^{III} product [(^{pR}N3C)Pd^{III}(MeCN)$_2$]$(BF_4)_2$, **2**. Combined experimental and computational data support that a CMD-like C–H bond activation constitutes the rate-determining step, in which a proposed Pd–superoxide species functionally acts as the base in a traditional CMD process. Water plays a critical role in lowering the activation barrier, enabling near-quantitative product formation, while O_2 acts as both oxidant and proton acceptor, producing H_2O_2 as the sole byproduct. A slight increase in reaction temperature substantially shortens the reaction time to under two hours, highlighting the practical viability of O_2 as a green oxidant for C–H bond activation under aqueous conditions.

Overall, this study establishes a mechanistically distinct and sustainable strategy for aerobic C–H bond activation that proceeds at a Pd center without an added external base. These findings provide fundamental insight into the design of aerobic oxidation processes under mild and environmentally benign conditions and further expand the scope of high-valent palladium chemistry.

Author contributions

D. Y. B. and L. M. M. conceptualized and designed the project. D. Y. B. and L. M. M. designed the experiments and computations. Experimental work was conducted by D. Y. B. and N. P. R., with N. P. R. contributing to the initial investigation. D. Y. B. and L. M. M. wrote the manuscript with input from all authors. L. M. M. directed the project.

Conflicts of interest

The authors have no conflicts to declare.

Data availability

CCDC 2331324 (for **1a**), 2331325 (for **1ab**) and 2331326 (for **2a**) contain the supplementary crystallographic data for this paper.[98a–c]

Supplementary information (SI): synthetic details, spectroscopic characterization, mechanistic and kinetic studies, crystallographic data, and computational details. See DOI: https://doi.org/10.1039/d6sc03081e.

Acknowledgements

This work was supported by the National Science Foundation (CHE-2102544 and CHE-2453341 to L. M. M.). We would like to thank the Department of Chemistry at the University of Illinois Urbana-Champaign for all the support. We also thank Drs Toby Woods, Danielle Gray, and Nigam Rath for help with X-ray crystal structure analysis, and Dr Lingyang Zhu for help with low-temperature NMR experiments. We thank Drs S. Chakrabarti, C.-H. Hu, J. B. Chae, and D. Jeong for helpful discussions related to this project.

References

1 T. W. Lyons and M. S. Sanford, Palladium-Catalyzed Ligand-Directed C-H Functionalization Reactions, *Chem. Rev.*, 2010, **110**, 1147–1169.
2 D. Kalyani, K. B. McMurtrey, S. R. Neufeldt and M. S. Sanford, Room-Temperature C-H Arylation: Merger of Pd-Catalyzed C-H Functionalization and Visible-Light Photocatalysis, *J. Am. Chem. Soc.*, 2011, **133**, 18566–18569.
3 K. M. Engle, T.-S. Mei, M. Wasa and J.-Q. Yu, Weak Coordination as a Powerful Means for Developing Broadly Useful C-H Functionalization Reactions, *Acc. Chem. Res.*, 2012, **45**, 788–802.
4 K. M. Engle and J.-Q. Yu, Developing Ligands for Palladium(II)-Catalyzed C-H Functionalization: Intimate Dialogue between Ligand and Substrate, *J. Org. Chem.*, 2013, **78**, 8927–8955.
5 I. A. Sanhueza, A. M. Wagner, M. S. Sanford and F. Schoenebeck, On the role of anionic ligands in the site-selectivity of oxidative C-H functionalization reactions of arenes, *Chem. Sci.*, 2013, **4**, 2767–2775.
6 J. J. Topczewski and M. S. Sanford, Carbon-hydrogen (C-H) bond activation at PdIV: a Frontier in C-H functionalization catalysis, *Chem. Sci.*, 2015, **6**, 70–76.
7 Q. Shao, K. Wu, Z. Zhuang, S. Qian and J. Q. Yu, From Pd(OAc)(2) to Chiral Catalysts: The Discovery and Development of Bifunctional Mono-N-Protected Amino Acid Ligands for Diverse C-H Functionalization Reactions, *Acc. Chem. Res.*, 2020, **53**, 833–851.
8 K. L. Hull, E. L. Lanni and M. S. Sanford, Highly Regioselective Catalytic Oxidative Coupling Reactions: Synthetic and Mechanistic Investigations, *J. Am. Chem. Soc.*, 2006, **128**, 14047–14049.
9 A. J. Canty, Organopalladium and platinum chemistry in oxidising milieu as models for organic synthesis involving the higher oxidation states of palladium, *J. Chem. Soc., Dalton Trans.*, 2009, 10409–10417.
10 X. Chen, K. M. Engle, D. H. Wang and J. Q. Yu, Palladium(II)-Catalyzed C-H Activation/C-C Cross-Coupling Reactions: Versatility and Practicality, *Angew. Chem., Int. Ed.*, 2009, **48**, 5094–5115.
11 K. Muñiz, High-Oxidation-State Palladium Catalysis: New Reactivity for Organic Synthesis, *Angew. Chem., Int. Ed.*, 2009, **48**, 9412–9423.
12 P. Sehnal, R. J. K. Taylor and I. J. S. Fairlamb, Emergence of Palladium(IV) Chemistry in Synthesis and Catalysis, *Chem. Rev.*, 2010, **110**, 824–889.
13 D. C. Powers and T. Ritter, Palladium(III) in Synthesis and Catalysis, *Top. Organomet. Chem.*, 2011, **35**, 129–156.
14 W. Zhou, S. A. Zheng, J. W. Schultz, N. P. Rath and L. M. Mirica, Aromatic Cyanoalkylation through Double C-H Activation Mediated by Ni(III), *J. Am. Chem. Soc.*, 2016, **138**, 5777–5780.
15 N. P. Ruhs, J. Khusnutdinova, N. P. Rath and L. M. Mirica, Mononuclear Organometallic Pd(II), Pd(III), and Pd(IV) Complexes Stabilized by a Pyridinophane Ligand with a C-Donor Group, *Organometallics*, 2019, **38**, 3834–3843.
16 J. J. N. Leung, D. Y. Bae, Y. Moshood and L. M. Mirica, C-C and C-O bond formation reactivity of nickel complexes supported by the pyridinophane N3C ligand, *Dalton Trans.*, 2025, **54**, 5286–5292.
17 S. Chakrabarti, S. Sinha, G. N. Tran, H. Na and L. M. Mirica, Characterization of paramagnetic states in an organometallic nickel hydrogen evolution electrocatalyst, *Nat. Commun.*, 2023, **14**, 905.
18 B. S. Bouley, F. Z. Tang, D. Y. Bae and L. M. Mirica, C-H bond activation via concerted metalation-deprotonation at a palladium(III) center, *Chem. Sci.*, 2023, **14**, 3800–3808.
19 S. M. Smith, O. Planas, L. Gomez, N. Rath, X. Ribas and L. M. Mirica, Aerobic C-C and C-O bond formation reactions mediated by high-valent nickel species, *Chem. Sci.*, 2019, **10**, 10366–10372.
20 W. Zhou, N. P. Rath and L. M. Mirica, Oxidatively-induced aromatic cyanation mediated by Ni(III), *Dalton Trans.*, 2016, **45**, 8693–8695.
21 N. R. Deprez and M. S. Sanford, Reactions of hypervalent iodine reagents with palladium: Mechanisms and applications in organic synthesis, *Inorg. Chem.*, 2007, **46**, 1924–1935.
22 K. M. Engle, T. S. Mei, X. S. Wang and J. Q. Yu, Bystanding F(+) Oxidants Enable Selective Reductive Elimination from High-Valent Metal Centers in Catalysis, *Angew. Chem., Int. Ed.*, 2011, **50**, 1478–1491.
23 B. M. Stoltz, Palladium catalyzed aerobic dehydrogenation: from alcohols to indoles and asymmetric catalysis, *Chem. Lett.*, 2004, **33**, 362–367.
24 S. S. Stahl, Palladium oxidase catalysis. Selective oxidation of organic chemicals by direct dioxygen-coupled turnover, *Angew. Chem., Int. Ed.*, 2004, **43**, 3400–3420.
25 S. S. Stahl, Palladium-catalyzed oxidation of organic chemicals with O_2, *Science*, 2005, **309**, 1824–1826.

26 E. M. Beck, N. P. Grimster, R. Hatley and M. J. Gaunt, Mild Aerobic Oxidative Palladium (II) Catalyzed C−H Bond Functionalization: Regioselective and Switchable C−H Alkenylation and Annulation of Pyrroles, *J. Am. Chem. Soc.*, 2006, **128**, 2528–2529.
27 M. S. Sigman and D. R. Jensen, Ligand-Modulated Palladium-Catalyzed Aerobic Alcohol Oxidations, *Acc. Chem. Res.*, 2006, **39**, 221–229.
28 K. M. Gligorich and M. S. Sigman, Recent advancements and challenges of palladium(II)-catalyzed oxidation reactions with molecular oxygen as the sole oxidant, *Chem. Commun.*, 2009, 3854–3867.
29 A. N. Campbell and S. S. Stahl, Overcoming the "Oxidant Problem": Strategies to Use O2 as the Oxidant in Organometallic Câ€“H Oxidation Reactions Catalyzed by Pd (and Cu), *Acc. Chem. Res.*, 2012, **45**, 851–863.
30 A. N. Vedernikov, Direct Functionalization of Mâ€“C (M = PtII, PdII) Bonds Using Environmentally Benign Oxidants, O2 and H2O2, *Acc. Chem. Res.*, 2012, **45**, 803–813.
31 S. Q. Qian, Z. Q. Li, M. Y. Li, S. R. Wisniewski, J. X. Qiao, J. M. Richter, W. R. Ewing, M. D. Eastgate, J. S. Chen and J. Q. Yu, Ligand-Enabled Pd(II)-Catalyzed C(sp(3))-H Lactonization Using Molecular Oxygen as Oxidant, *Org. Lett.*, 2020, **22**, 3960–3963.
32 H. M. Ibrahim and H. Behbehani, Palladium-Catalyzed Q-Tube-Assisted Protocol for Synthesizing Diaza-dibenzo[a,e] azulene and Diaza-benzo[a]fluorene Derivatives via O-2 Acid-Promoted Cross-Dehydrogenative Coupling, *J. Org. Chem.*, 2020, **85**, 15368–15381.
33 S. J. Tereniak and S. S. Stahl, Mechanistic Basis for Efficient, Site-Selective, Aerobic Catalytic Turnover in Pd-Catalyzed C-H Imidoylation of Heterocycle-Containing Molecules, *J. Am. Chem. Soc.*, 2017, **139**, 14533–14541.
34 D. Wang, A. B. Weinstein, P. B. White and S. S. Stahl, Ligand-Promoted Palladium-Catalyzed Aerobic Oxidation Reactions, *Chem. Rev.*, 2018, **118**, 2636–2679.
35 Z. Li, Z. Wang, N. Chekshin, S. Q. Qian, J. X. Qiao, P. T. Cheng, K. S. Yeung, W. R. Ewing and J. Q. Yu, A tautomeric ligand enables directed C-H hydroxylation with molecular oxygen, *Science*, 2021, **372**, 1452–1457.
36 Y.-H. Zhang and J.-Q. Yu, Pd(II)-catalyzed hydroxylation of arenes with 1 atm of O2 or air, *J. Am. Chem. Soc.*, 2009, **131**, 14654–14655.
37 B. R. Rosen, L. R. Simke, P. S. Thuy-Boun, D. D. Dixon, J. Q. Yu and P. S. Baran, C-H Functionalization Logic Enables Synthesis of (+)-Hongoquercin A and Related Compounds, *Angew. Chem., Int. Ed.*, 2013, **52**, 7317–7320.
38 C. I. Herrerias, X. Q. Yao, Z. P. Li and C. J. Li, Reactions of C-H bonds in water, *Chem. Rev.*, 2007, **107**, 2546–2562.
39 T. Dalton, T. Faber and F. Glorius, C-H Activation: Toward Sustainability and Applications, *ACS Cent. Sci.*, 2021, **7**, 245–261.
40 Y. Wang, X. Zhang, J. Zhang and G. Zhong, Nature's Blueprint: Chelation-Assisted C-H Functionalization for Selective and Efficient Reactions in Aqueous Media, *Isr. J. Chem*, 2023, **63**, e202300048.
41 T. A. Shah, T. Sarkar, S. Kar, P. K. Maharana, K. Talukdar and T. Punniyamurthy, Transition-Metal-Catalyzed Directed C-H Functionalization in/on Water, *Chem.–Asian J.*, 2024, **19**, e202300815.
42 K. M. Dawood and M. Alaasar, Transition-metal-catalyzed Heteroannulation Reactions in Aqueous Medium, *Asian J. Org. Chem.*, 2022, **11**, e202200331.
43 J. Zhang, E. Khaskin, N. P. Anderson, P. Y. Zavalij and A. N. Vedernikov, Catalytic aerobic oxidation of substituted 8-methylquinolines in PdII-2,6-pyridinedicarboxylic acid systems, *Chem. Commun.*, 2008, 3625–3627.
44 A. Wang, H. Jiang and H. Chen, Palladium-Catalyzed Diacetoxylation of Alkenes with Molecular Oxygen as Sole Oxidant, *J. Am. Chem. Soc.*, 2009, **131**, 3846–3847.
45 M.-K. Zhu, J.-F. Zhao and T.-P. Loh, Palladium-Catalyzed Oxime Assisted Intramolecular Dioxygenation of Alkenes with 1 atm of Air as the Sole Oxidant, *J. Am. Chem. Soc.*, 2010, **132**, 6284–6285.
46 L. Boisvert, M. C. Denney, H. S. Kloek and K. I. Goldberg, Insertion of Molecular Oxygen into a Palladium(II) Methyl Bond: A Radical Chain Mechanism Involving Palladium(III) Intermediates, *J. Am. Chem. Soc.*, 2009, **131**, 15802–15814.
47 G. J. Chuang, W. Wang, E. Lee and T. Ritter, A Dinuclear Palladium Catalyst for α-Hydroxylation of Carbonyls with O2, *J. Am. Chem. Soc.*, 2011, **133**, 1760–1762.
48 J. R. Khusnutdinova and L. M. Mirica, in *C-H Activation and Functionalization, Transition Metal Mediation*, Royal Society of Chemistry, 2012.
49 K. Inamoto, K. Nozawa and Y. Kondo, Palladium-Catalyzed C-H Cyclization in Water: A Milder Route to 2-Arylbenzothiazoles, *Synlett*, 2012, 1678–1682.
50 V. Dura-Vila, D. M. P. Mingos, R. Vilar, A. J. P. White and D. J. Williams, Insertion of O2 into a Pd(I)-Pd(I) dimer and subsequent C-O bond formation by activation of a C-H bond, *Chem. Commun.*, 2000, 1525–1526.
51 M. L. Scheuermann, D. W. Boyce, K. A. Grice, W. Kaminsky, S. Stoll, W. B. Tolman, O. Swang and K. I. Goldberg, Oxygen-Promoted C-H Bond Activation at Palladium, *Angew. Chem., Int. Ed.*, 2014, **53**, 6492–6495.
52 J. R. Khusnutdinova, N. P. Rath and L. M. Mirica, The Aerobic Oxidation of a Pd(II) Dimethyl Complex Leads to Selective Ethane Elimination from a Pd(III) Intermediate, *J. Am. Chem. Soc.*, 2012, **134**, 2414–2422.
53 F. Tang, Y. Zhang, N. P. Rath and L. M. Mirica, Detection of Pd(III) and Pd(IV) Intermediates during the Aerobic Oxidative C-C Bond Formation from a Pd(II) Dimethyl Complex, *Organometallics*, 2012, **31**, 6690–6696.
54 J. W. Schultz, N. P. Rath and L. M. Mirica, Improved Oxidative C–C Bond Formation Reactivity of High-Valent Pd Complexes Supported by a Pseudo-Tridentate Ligand, *Inorg. Chem.*, 2020, **59**, 11782–11792.
55 F. Qu, J. R. Khusnutdinova, N. P. Rath and L. M. Mirica, Dioxygen activation by an organometallic Pd(II) precursor: formation of a Pd(IV)-OH complex and its C-O bond formation reactivity, *Chem. Commun.*, 2014, **50**, 3036–3039.

56 J. R. Khusnutdinova, F. Qu, Y. Zhang, N. P. Rath and L. M. Mirica, Formation of the Pd(IV) Complex [(Me_3tacn)$Pd^{IV}Me_3$]$^+$ through Aerobic Oxidation of (Me_3tacn)$Pd^{II}Me_2$ (Me_3tacn = N,N',N''-trimethyl-1,4,7-triazacyclononane), *Organometallics*, 2012, **31**, 4627–4630.

57 M. Brookhart, M. L. H. Green and G. Parkin, Agostic interactions in transition metal compounds, *Proc. Natl. Acad. Sci. U. S. A.*, 2007, **104**, 6908–6914.

58 J. P. Stambuli, C. D. Incarvito, M. Bühl and J. F. Hartwig, Synthesis, Structure, Theoretical Studies, and Ligand Exchange Reactions of Monomeric, T-Shaped Arylpalladium(II) Halide Complexes with an Additional, Weak Agostic Interaction, *J. Am. Chem. Soc.*, 2004, **126**, 1184–1194.

59 L. H. Shultz and M. Brookhart, Measurement of the Barrier to β-Hydride Elimination in a β-Agostic Palladium−Ethyl Complex: A Model for the Energetics of Chain-Walking in (α-Diimine)PdR+ Olefin Polymerization Catalysts, *Organometallics*, 2001, **20**, 3975–3982.

60 A. Vigalok, O. Uzan, L. J. W. Shimon, Y. Ben-David, J. M. L. Martin and D. Milstein, Formation of η2 C−H Agostic Rhodium Arene Complexes and Their Relevance to Electrophilic Bond Activation, *J. Am. Chem. Soc.*, 1998, **120**, 12539–12544.

61 A. Poater, X. Solans-Monfort, E. Clot, C. Coperet and O. Eisenstein, DFT calculations of d0 M(NR)(CHtBu)(X)(Y) (M = Mo, W; R = CPh3, 2,6-iPr-C6H3; X and Y = CH2tBu, OtBu, OSi(OtBu)3) olefin metathesis catalysts: structural, spectroscopic and electronic properties, *Dalton Trans.*, 2006, **35**, 3077–3087.

62 J. R. Khusnutdinova, N. P. Rath and L. M. Mirica, Stable Mononuclear Organometallic Pd(III) Complexes and Their C-C Bond Formation Reactivity, *J. Am. Chem. Soc.*, 2010, **132**, 7303–7305.

63 F. Z. Tang, F. R. Qu, J. R. Khusnutdinova, N. P. Rath and L. M. Mirica, Structural and reactivity comparison of analogous organometallic Pd(III) and Pd(IV) complexes, *Dalton Trans.*, 2012, **41**, 14046–14050.

64 J. R. Khusnutdinova, N. P. Rath and L. M. Mirica, The Conformational Flexibility of the Tetradentate Ligand ^{tBu}N4 is Essential for the Stabilization of (^{tBu}N4)Pd^{III} Complexes, *Inorg. Chem.*, 2014, **53**, 13112–13129.

65 N. G. Connelly and W. E. Geiger, Chemical Redox Agents for Organometallic Chemistry, *Chem. Rev.*, 1996, **96**, 877–910.

66 Tania, T. B. Poynder, A. Kaur, L. Barwise, S. D. Houston, A. J. Nair, J. K. Clegg, D. J. D. Wilson and J. L. Dutton, PhICl(2) is activated by chloride ions, *Dalton Trans.*, 2021, **50**, 11986–11991.

67 M. L. Pegis, C. F. Wise, D. J. Martin and J. M. Mayer, Oxygen Reduction by Homogeneous Molecular Catalysts and Electrocatalysts, *Chem. Rev.*, 2018, **118**, 2340–2391.

68 J. Casado, M. A. Lopezquintela and F. M. Lorenzobarral, The Initial Rate Method in Chemical-Kinetics - Evaluation and Experimental Illustration, *J. Chem. Educ.*, 1986, **63**, 450–452.

69 J. M. Achord and C. L. Hussey, Determination of dissolved oxygen in nonaqueous electrochemical solvents, *Anal. Chem.*, 1980, **52**, 601–602.

70 C. Franco and J. Olmsted, Photochemical determination of the solubility of oxygen in various media, *Talanta*, 1990, **37**, 905–909.

71 E. M. Simmons and J. F. Hartwig, On the Interpretation of Deuterium Kinetic Isotope Effects in C–H Bond Functionalizations by Transition-Metal Complexes, *Angew. Chem., Int. Ed.*, 2012, **51**, 3066–3072.

72 A. D. Ryabov, I. K. Sakodinskaya and A. K. Yatsimirsky, Kinetics and mechanism of ortho-palladation of ring-substituted NN-dimethylbenzylamines, *J. Chem. Soc., Dalton Trans.*, 1985, 2629–2638.

73 A. D. Ryabov, Mechanisms of intramolecular activation of carbon-hydrogen bonds in transition-metal complexes, *Chem. Rev.*, 1990, **90**, 403–424.

74 A. D. Ryabov, I. K. Sakodinskaya and A. K. Yatsimirsky, Comparative study of the mechanism of alkynelation of ortho-palladated benzylamines and acetanilides, *J. Organomet. Chem.*, 1991, **406**, 309–321.

75 D. Lapointe and K. Fagnou, Overview of the Mechanistic Work on the Concerted Metallation–Deprotonation Pathway, *Chem. Lett.*, 2010, **39**, 1118–1126.

76 K. M. Altus and J. A. Love, The continuum of carbon-hydrogen (C-H) activation mechanisms and terminology, *Commun. Chem.*, 2021, **4**, 713.

77 D. L. Davies, S. A. Macgregor and C. L. McMullin, Computational Studies of Carboxylate-Assisted C–H Activation and Functionalization at Group 8–10 Transition Metal Centers, *Chem. Rev.*, 2017, **117**, 8649–8709.

78 D. L. Davies, S. M. A. Donald and S. A. Macgregor, Computational Study of the Mechanism of Cyclometalation by Palladium Acetate, *J. Am. Chem. Soc.*, 2005, **127**, 13754–13755.

79 M. D. K. Boele, G. P. F. van Strijdonck, A. H. M. de Vries, P. C. J. Kamer, J. G. de Vries and P. W. N. M. van Leeuwen, Selective Pd-Catalyzed Oxidative Coupling of Anilides with Olefins through C−H Bond Activation at Room Temperature, *J. Am. Chem. Soc.*, 2002, **124**, 1586–1587.

80 F. Z. Tang, N. P. Rath and L. M. Mirica, Stable bis(trifluoromethyl)nickel(III) complexes, *Chem. Commun.*, 2015, **51**, 3113–3116.

81 A. Rana, Y. M. Lee, X. L. Li, R. Cao, S. Fukuzumi and W. Nam, Highly Efficient Catalytic Two-Electron Two-Proton Reduction of Dioxygen to Hydrogen Peroxide with a Cobalt Corrole Complex, *ACS Catal.*, 2021, **11**, 3073–3083.

82 Y. H. Wang, B. Mondal and S. S. Stahl, Molecular Cobalt Catalysts for O2 Reduction to H2O: Benchmarking Catalyst Performance via Rate-Overpotential Correlations, *ACS Catal.*, 2020, **10**, 12031–12039.

83 S. D. McCann and S. S. Stahl, Copper-Catalyzed Aerobic Oxidations of Organic Molecules: Pathways for Two-Electron Oxidation with a Four-Electron Oxidant and a One-Electron Redox-Active Catalyst, *Acc. Chem. Res.*, 2015, **48**, 1756–1766.

84 Y. Lee, G. Y. Park, H. R. Lucas, P. L. Vajda, K. Kamaraj, M. A. Vance, A. E. Milligan, J. S. Woertink, M. A. Siegler, A. A. N. Sarjeant, L. N. Zakharov, A. L. Rheingold, E. I. Solomon and K. D. Karlin, Copper(I)/O2 Chemistry

with Imidazole Containing Tripodal Tetradentate Ligands Leading to μ-1,2-Peroxo-Dicopper(II) Species, *Inorg. Chem.*, 2009, **48**, 11297–11309.

85 V. P. Ananikov, Nickel: The "Spirited Horse" of Transition Metal Catalysis, *ACS Catal.*, 2015, **5**, 1964–1971.

86 G. M. Eisenberg, Colorimetric determination of hydrogen peroxide, *Ind. Eng. Chem., Anal. Ed.*, 1943, **15**, 327–328.

87 A. Kunishita, M. Z. Ertem, Y. Okubo, T. Tano, H. Sugimoto, K. Ohkubo, N. Fujieda, S. Fukuzumi, C. J. Cramer and S. Itoh, Active Site Models for the Cu Site of Peptidylglycine α-Hydroxylating Monooxygenase and Dopamine β-Monooxygenase, *Inorg. Chem.*, 2012, **51**, 9465–9480.

88 S. Y. Quek, S. Debnath, S. Laxmi, M. Van Gastel, T. Kramer and J. England, Sterically Stabilized End-On Superoxocopper(II) Complexes and Mechanistic Insights into Their Reactivity with O-H, N-H, and C-H Substrates, *J. Am. Chem. Soc.*, 2021, **143**, 19731–19747.

89 K. B. Cho, H. Kang, J. Woo, Y. J. Park, M. S. Seo, J. Cho and W. Nam, Mechanistic Insights into the C-H Bond Activation of Hydrocarbons by Chromium(IV) Oxo and Chromium(III) Superoxo Complexes, *Inorg. Chem.*, 2014, **53**, 645–652.

90 T. Wada, H. Sugimoto, Y. Morimoto and S. Itoh, Alkane hydroxylation by a-chloroperbenzoic acid catalyzed by nickel(II) complexes of linear N-tetradentate ligands, *Polyhedron*, 2022, 227.

91 C. H. Hu, S. T. Kim, M. H. Baik and L. M. Mirica, Nickel-Carbon Bond Oxygenation with Green Oxidants via High-Valent Nickel Species, *J. Am. Chem. Soc.*, 2023, **145**, 11161–11172.

92 A. Maleckis, J. W. Kampf and M. S. Sanford, A Detailed Study of Acetate-Assisted C–H Activation at Palladium(IV) Centers, *J. Am. Chem. Soc.*, 2013, **135**, 6618–6625.

93 A. McAuley and T. W. Whitcombe, Bis(1,4,7-triazacyclononane)palladium(III): characterization and reactions of an unusually stable monomeric palladium(III) ion, *Inorg. Chem.*, 1988, **27**, 3090–3099.

94 L. M. Mirica and J. R. Khusnutdinova, Structure and electronic properties of Pd(III) complexes, *Coord. Chem. Rev.*, 2013, **257**, 299–314.

95 S. Sinha and L. M. Mirica, Electrocatalytic O2 Reduction by an Organometallic Pd(III) Complex via a Binuclear Pd(III) Intermediate, *ACS Catal.*, 2021, **11**, 5202–5211.

96 S. Yamaguchi, S. Nagatomo, T. Kitagawa, Y. Funahashi, T. Ozawa, K. Jitsukawa and H. Masuda, Copper hydroperoxo species activated by hydrogen-bonding interaction with its distal oxygen, *Inorg. Chem.*, 2003, **42**, 6968–6970.

97 W. Rauf and J. M. Brown, Palladium-catalysed directed C-H activation by anilides and ureas; water participation in a general base mechanism, *Org. Biomol. Chem.*, 2016, **14**, 5251–5257.

98 (*a*) CCDC 2331324: Experimental Crystal Structure Determination, 2026, DOI: 10.5517/ccdc.csd.cc2j7y0r; (*b*) CCDC 2331325: Experimental Crystal Structure Determination, 2026, DOI: 10.5517/ccdc.csd.cc2j7y1s; (*c*) CCDC 2331326: Experimental Crystal Structure Determination, 2026, DOI: 10.5517/ccdc.csd.cc2j7y2t.